recently reported to be important for HCV infection by Vanwolleghem *et al.*,[47] who showed that 100% HCV infectivity was reached with high quality inocula in mice with human albumin levels of more than 1 mg/mL.

Spontaneous eradication of HCV has been reported to be higher in individuals with the rs12979860CC genotype.[20] In such individuals, components of both the innate and adaptive immune systems likely play a role in eliminating the invading virus in the absence of exogenous IFN. As no human or mouse adaptive immune effector cells are present in human hepatocyte chimeric mice, it is possible to isolate the effects of innate immunity in liver cells using this model. When liver cells are selected from donors with different *IL-28B* genotypes, the model provides an opportunity to study differences in innate immune responses associated with the *IL-28B* genotype.

Clonal infection with HCV genotypes 1a, 1b, 2a and 2b is now possible,[48–50] and reverse genetic approaches combining infectious HCV clones with the human hepatocyte chimeric mouse facilitate studying the effects of viral mutations and host factors, such as the *IL-28B* genotype, on infectivity of the virus. Several factors may influence infectivity of the virus, including serum lipid profile,[51] presence of neutralizing antibodies and presence of antibody-resistant viral quasispecies.[52,53] However, we found no difference in incidence of establishment of infection with genotype 1b clones among mice transplanted with different *IL-28B* genotype liver cells.[54] This result may derive from the specific infection route (intrahepatic injection of RNA to mouse liver) and the large RNA titers used in the study.

EXPRESSION OF INTERFERON-STIMULATED GENE (ISG) AND VIRAL LOAD IN HUMANS AND HUMAN HEPATOCYTE CHIMERIC MICE

ALTHOUGH THE MECHANISM underlying the *IL-28B* polymorphism remains unclear, a number of studies have reported that intrahepatic ISG expression levels are lower[55–57] and viral titers are higher[8,12] in patients with the eradication-favorable *IL-28B* genotype. Honda *et al.* showed that expression of a number of ISGs was higher in patients with the unfavorable rs8099917 TG or GG genotypes compared to those with the TT genotype and that non-responders were significantly over-represented among patients with high ISG expression levels.[57] Using paired liver biopsy samples, Sarasin-Filipowicz demonstrated that ISG expression levels in non-responders were initially higher prior to IFN treatment, but administration of IFN failed to induce ISG expression levels above this baseline level, whereas IFN induced a strong upregulation of ISG expression in patients who achieved a rapid virological response.[58] Shebl *et al.* measured ISG expression levels in uninfected cells and found no evidence of an association with the *IL-28B* genotype, suggesting that the association observed in HCV-infected cells does not reflect normal expression levels in healthy cells and reflects the response to HCV infection.[59]

The chimeric mouse provides a suitable model to test hypotheses concerning the role of the *IL-28B* genotype on innate immune responses and ISG expression. Using this model, we found that ISG expression levels were also lower and viral titers were higher in human hepatocyte chimeric mice with the favorable *IL-28B* genotype.[54] As illustrated in Figure 1, the virus appears to replicate more efficiently in mice with the favorable genotype, perhaps because whenever the viral load is low hepatocytes with the favorable genotype can efficiently clear the virus so that chronic infection only results under higher viral loads.[20,60] At the same time, ISG expression is lower in cells with the favorable allele, which may be advantageous by preventing saturation of the IFN signaling pathway through continual stimulation.[58] However, earlier reports demonstrated that induction of a strong response to IFN-α is dependent on a weak constitutive IFN signal to maintain IFN-dependent expression of insulin-related factor-7, an essential transcription factor involved in IFN signal transduction that has a short half-life.[61] The unfavorable *IL-28B* genotype might alter the balance of this feedback loop in the presence of HCV. Although we observed that ISG expression levels were lower in mice with the favorable genotype prior to IFN treatment (unpubl. data, K. Chayama, Hiroshima University, Japan), ISG expression increased sharply following IFN administration in mice with the favorable genotype and were significantly higher than in mice with an unfavorable genotype.[54]

ISG EXPRESSION LEVELS AND EFFECT OF IFN THERAPY IN HUMANS AND CHIMERIC MICE

PRETREATMENT ISG EXPRESSION levels may be a stronger predictor of outcome of combination therapy than the *IL-28B* genotype,[62] suggesting that the mechanism of the SNP is related to its role in ISG regulation. Lower ISG expression levels are associated with the eradication-favorable *IL-28B* genotype in chronic hepatitis C patients,[55–57] and high baseline expression levels of ISG such as *RIG-I*, *ISG-15* and *USP-18* correlate with poor response to therapy.[63] Using the human

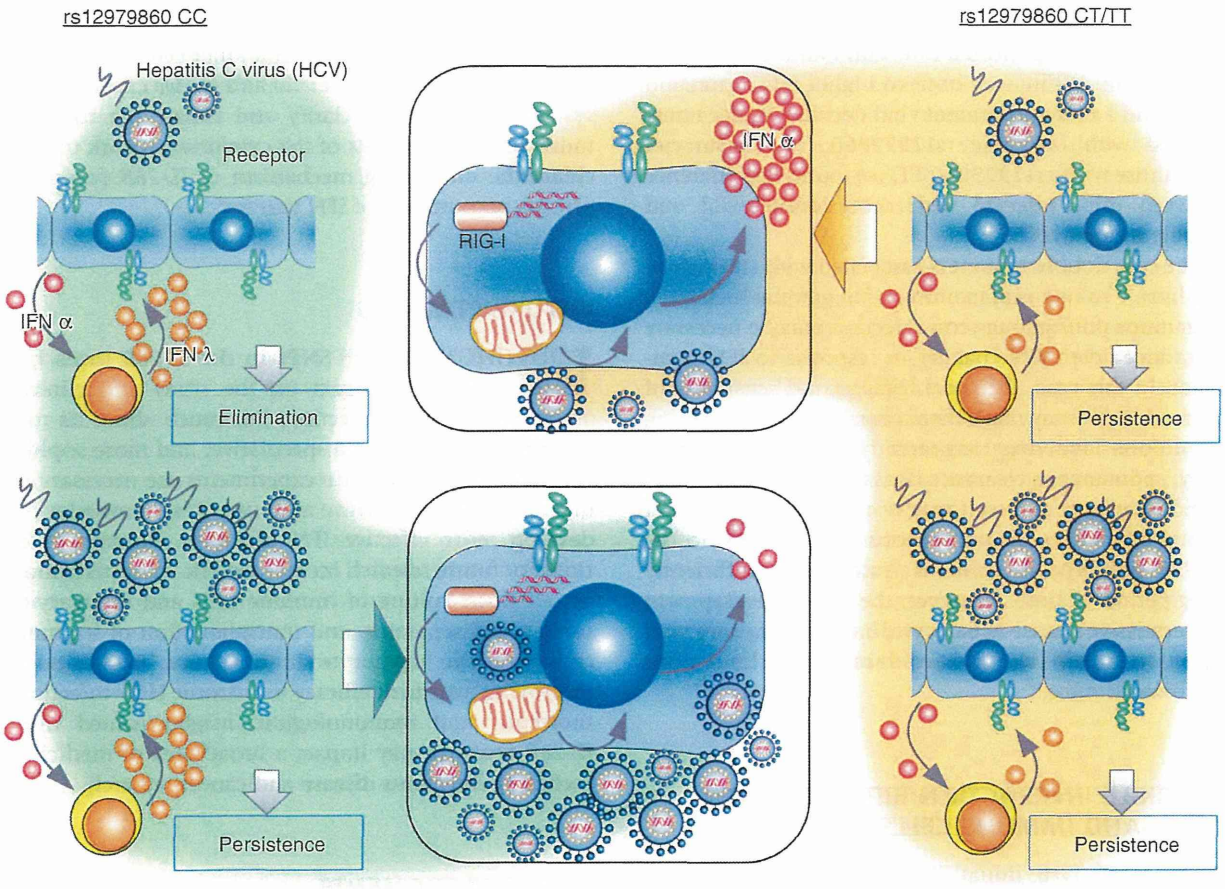

Figure 1 Hypothetical model of virus replication in hepatocytes with eradication-favorable (interleukin [IL]-28B rs12979860 CC or rs8099917 TT) or unfavorable (rs12979860 CT/TT or rs8099917 GT/GG) genotypes. HCV may be eliminated from individuals with the favorable genotype at low titer but may persistently infect those with high titers or the unfavorable genotype (upper right and left panels). Viral sensors continuously detect viral RNA during chronic infection (central panel), resulting in continuous activation of interferon-stimulated genes (ISG), including interferon inhibitory molecules such as *PIAS* and SOCS3. In hepatocytes with the unfavorable genotype, ISG expression may be refractory to further interferon stimulation, resulting in a poor response to therapy, but in hepatocytes with the favorable genotype, low baseline ISG expression may prevent overexpression of interferon signal inhibitors, resulting in stronger ISG induction and a better response to therapy.

hepatocyte chimeric mouse model, we showed that intrahepatic expression levels were significantly higher and HCV RNA reduction was significantly greater in mice with rs12979860CC hepatocytes following IFN administration.[54] Several genes that suppress IFN-dependent antiviral activity, such as *PIAS* and genes in the SOCS family, are themselves ISGs, and may serve as a negative feedback loop to regulate IFN signaling. Consequently, continuous low-level ISG expression in hepatocytes with the unfavorable genotype may dampen IFN sensitivity and prevent effective ISG induction when IFN is administrated during treatment.

RELATIONSHIP BETWEEN *IL-28B* GENOTYPE AND HCV CORE AMINO ACID SUBSTITUTIONS

REVERSE GENETICS USING the chimeric mouse model could facilitate detailed studies of the effect of host and viral factors on IFN sensitivity and ISG expression. HCV core protein substitutions are predictive of outcome of peginterferon plus ribavirin combination therapy,[64,65] and patients with the unfavorable *IL-28B* genotype are more likely to host viruses having core substitutions.[66] To examine these interactions *in*

vivo, we created core amino acid 70 and 91 double wild and double mutant clones using the infectious genotype clone KT-9 and performed infection and IFN treatment experiments. While we observed higher ISG expression levels and a more prominent viral decline in mice transplanted with favorable rs12979860 CC hepatocytes than those with rs12979860 TT, we found no difference between mice infected with core double wild and double mutant HCV.[54]

The core double mutant is associated with steatosis of the liver,[67] so one explanation is that gradual metabolic alterations during long-term infection may be necessary to induce detectable changes in response to IFN treatment. In this case, the short lifespan and sensitivity of chimeric mice may make them unsuitable for examining conditions involving long-term hepatic change. Similarly, spontaneous clearance does not necessarily imply rapid clearance, and so it may not be possible to detect subtle differences in spontaneous clearance due to the *IL-28B* genotype in chimeric mice over a sufficiently long period of time. However, the recent development of permissive mouse hepatocyte lines may improve viral infection rates in mice and avoid some of the limitations of chimeric mice.[68]

POSSIBLE INTERACTION BETWEEN LIVER CELLS AND IMMUNE CELLS

TWO OF THE initial *IL-28B* reports showed that production of IL-28 was higher in individual leukocytes homozygous for the eradication-favorable allele (rs12979860 CC or rs8099917 TT),[8,10] suggesting that stronger IFN-λ expression was responsible for the better response to therapy, although Urban *et al.* found no association between *IL-28B* genotype and *IL-28B* or *IL-28A* expression.[56] Honda *et al.* also found no association between *IL-28B* genotype and *IL-28B* expression, although they point out that it may be difficult to detect differences in expression levels due to the high sequence similarity between *IL-28A* and *IL-28B* and the relatively low expression levels of these genes regardless of genotype.[57] Although IFN-λ inhibits replication of HCV genotypes 1 and 2[69] and induces essentially the same set of ISGs as IFN-α,[62] IFN-λ may act synergistically by enhancing the antiviral efficacy of sub-saturating levels of IFN-α.[69] IFN-α and IFN-λ also have different kinetics. Marcello *et al.* showed that IFN-α induces an early peak followed by a rapid decline, whereas IFN-λ induces slower but more sustained ISG expression.[69] Therefore, coordination of autocrine and paracrine IFN expression is likely complex and may involve interactions between hepatocytes and immune cells such as dendritic cells, cytotoxic T lymphocytes, natural killer cells and natural killer T cells. The use of *in vitro* and *in vivo* experimental systems may help to clarify and isolate the roles of individual components of the cytokine network to elucidate the underlying mechanism of *IL-28B* polymorphisms on outcome of IFN therapy.

FUTURE REMARKS

IDENTIFICATION OF SNPs in the *IL-28B* locus has had a dramatic impact on the study and clinical assessment of HCV infection, but much about its role remains paradoxical and speculative, and more sophisticated *in vitro* and *in vivo* experiments are necessary to uncover the mechanism and use this knowledge to develop more effective IFN therapies. Recommendations for future research include genetic characterization of cell lines, culture of immune cells and hepatocytes using a cell separator, and transplantation of immune cells to human hepatocyte chimeric mice. In addition to improving treatment efficacy for chronic HCV infection, molecular and immunological insights gained from *IL-28B* research may impact a broad area of medicine, including infectious disease and cancer research.

ACKNOWLEDGMENTS

THIS WORK WAS supported in part by Grants-in-Aid for scientific research and development from the Ministry of Education, Culture, Sports, Science and Technology, and the Ministry of Health, Labor and Welfare, Government of Japan.

REFERENCES

1 Ank N, Iversen MB, Bartholdy C *et al.* An important role for type III interferon (IFN-lambda/IL-28) in TLR-induced antiviral activity. *J Immunol* 2008; **180**: 2474–85.
2 Bartlett NW, Buttigieg K, Kotenko SV, Smith GL. Murine interferon lambdas (type III interferons) exhibit potent antiviral activity in vivo in a poxvirus infection model. *J Gen Virol* 2005; **86**: 1589–96.
3 Brand S, Beigel F, Olszak T *et al.* IL-28A and IL-29 mediate antiproliferative and antiviral signals in intestinal epithelial cells and murine CMV infection increases colonic IL-28A expression. *Am J Physiol Gastrointest Liver Physiol* 2005; **289**: G960–8.

4 Doyle SE, Schreckhise H, Khuu-Duong K *et al.* Interleukin-29 uses a type 1 interferon-like program to promote antiviral responses in human hepatocytes. *Hepatology* 2006; **44**: 896–906.
5 Fox BA, Sheppard PO, O'Hara PJ. The role of genomic data in the discovery, annotation and evolutionary interpretation of the interferon-lambda family. *PLoS ONE* 2009; **4**: e4933.
6 Meager A, Visvalingam K, Dilger P, Bryan D, Wadhwa M. Biological activity of interleukins-28 and -29: comparison with type I interferons. *Cytokine* 2005; **31**: 109–18.
7 Sheppard P, Kindsvogel W, Xu W *et al.* IL-28, IL-29 and their class II cytokine receptor IL-28R. *Nat Immunol* 2003; **4**: 63–8.
8 Ge D, Fellay J, Thompson AJ *et al.* Genetic variation in IL28B predicts hepatitis C treatment-induced viral clearance. *Nature* 2009; **461**: 399–401.
9 Tanaka Y, Nishida N, Sugiyama M *et al.* Genome-wide association of IL28B with response to pegylated interferon-alpha and ribavirin therapy for chronic hepatitis C. *Nat Genet* 2009; **41**: 1105–9.
10 Suppiah V, Moldovan M, Ahlenstiel G *et al.* IL28B is associated with response to chronic hepatitis C interferon-alpha and ribavirin therapy. *Nat Genet* 2009; **41**: 1100–4.
11 Rauch A, Kutalik Z, Descombes P *et al.* Genetic variation in IL28B is associated with chronic hepatitis C and treatment failure: a genome-wide association study. *Gastroenterology* 2010; **138**: 1338–45. 45 e1-7.
12 Ochi H, Maekawa T, Abe H *et al.* IL-28B predicts response to chronic hepatitis C therapy -fine-mapping and replication study in Asian populations. *J Gen Virol* 2011; **92**: 1071–81.
13 Moghaddam A, Melum E, Reinton N *et al.* IL28B genetic variation and treatment response in patients with hepatitis C virus genotype 3 infection. *Hepatology* 2011; **53**: 746–54.
14 Sakamoto N, Nakagawa M, Tanaka Y *et al.* Association of IL28B variants with response to pegylated-interferon alpha plus ribavirin combination therapy reveals intersubgenotypic differences between genotypes 2a and 2b. *J Med Virol* 2011; **83**: 871–8.
15 Yu ML, Huang CF, Huang JF *et al.* Role of interleukin-28B polymorphisms in the treatment of hepatitis C virus genotype 2 infection in Asian patients. *Hepatology* 2011; **53**: 7–13.
16 Scherzer TM, Hofer H, Staettermayer AF *et al.* Early virologic response and IL28B polymorphisms in patients with chronic hepatitis C genotype 3 treated with peginterferon alfa-2a and ribavirin. *J Hepatol* 2011; **54**: 866–71.
17 Kawaoka T, Hayes CN, Ohishi W *et al.* Predictive value of the IL28B polymorphism on the effect of interferon therapy in chronic hepatitis C patients with genotypes 2a and 2b. *J Hepatol* 2011; **54**: 408–14.
18 Sarrazin C, Susser S, Doehring A *et al.* Importance of IL28B gene polymorphisms in hepatitis C virus genotype 2 and 3 infected patients. *J Hepatol* 2011; **54**: 415–21.
19 Mangia A, Thompson AJ, Santoro R *et al.* An IL28B polymorphism determines treatment response of hepatitis C virus genotype 2 or 3 patients who do not achieve a rapid virologic response. *Gastroenterology* 2010; **139**: 821–7, 7 e1.
20 Thomas DL, Thio CL, Martin MP *et al.* Genetic variation in IL28B and spontaneous clearance of hepatitis C virus. *Nature* 2009; **461**: 798–801.
21 Tillmann HL, Thompson AJ, Patel K *et al.* A polymorphism near IL28B is associated with spontaneous clearance of acute hepatitis C virus and jaundice. *Gastroenterology* 2010; **139**: 1586–92, 92 e1.
22 Bartenschlager R, Pietschmann T. Efficient hepatitis C virus cell culture system: what a difference the host cell makes. *Proc Natl Acad Sci U S A* 2005; **102**: 9739–40.
23 Wakita T, Pietschmann T, Kato T *et al.* Production of infectious hepatitis C virus in tissue culture from a cloned viral genome. *Nat Med* 2005; **11**: 791–6.
24 Zhong J, Gastaminza P, Cheng G *et al.* Robust hepatitis C virus infection in vitro. *Proc Natl Acad Sci U S A* 2005; **102**: 9294–9.
25 Sumpter R, Jr, Loo YM, Foy E *et al.* Regulating intracellular antiviral defense and permissiveness to hepatitis C virus RNA replication through a cellular RNA helicase, RIG-I. *J Virol* 2005; **79**: 2689–99.
26 Pileri P, Uematsu Y, Campagnoli S *et al.* Binding of hepatitis C virus to CD81. *Science* 1998; **282**: 938–41.
27 Durantel D, Zoulim F. Going towards more relevant cell culture models to study the in vitro replication of serum-derived hepatitis C virus and virus/host cell interactions? *J Hepatol* 2007; **46**: 1–5.
28 Ploss A, Khetani SR, Jones CT *et al.* Persistent hepatitis C virus infection in microscale primary human hepatocyte cultures. *Proc Natl Acad Sci U S A* 2010; **107**: 3141–5.
29 Narbus CM, Israelow B, Sourisseau M *et al.* HepG2 cells expressing MicroRNA miR-122 support the entire hepatitis C virus life cycle. *J Virol* 2011; **85**: 12087–92.
30 Kotenko SV, Gallagher G, Baurin VV *et al.* IFN-lambdas mediate antiviral protection through a distinct class II cytokine receptor complex. *Nat Immunol* 2003; **4**: 69–77.
31 Donnelly RP, Sheikh F, Kotenko SV, Dickensheets H. The expanded family of class II cytokines that share the IL-10 receptor-2 (IL-10R2) chain. *J Leukoc Biol* 2004; **76**: 314–21.
32 Dumoutier L, Tounsi A, Michiels T, Sommereyns C, Kotenko SV, Renauld JC. Role of the interleukin (IL)-28 receptor tyrosine residues for antiviral and antiproliferative activity of IL-29/interferon-lambda 1: similarities with type I interferon signaling. *J Biol Chem* 2004; **279**: 32269–74.
33 Brand S, Zitzmann K, Dambacher J *et al.* SOCS-1 inhibits expression of the antiviral proteins 2',5'-OAS and MxA induced by the novel interferon-lambdas IL-28A and IL-29. *Biochem Biophys Res Commun* 2005; **331**: 543–8.
34 Siren J, Pirhonen J, Julkunen I, Matikainen S. IFN-alpha regulates TLR-dependent gene expression of IFN-alpha, IFN-beta, IL-28, and IL-29. *J Immunol* 2005; **174**: 1932–7.

35 Mennechet FJ, Uze G. Interferon-lambda-treated dendritic cells specifically induce proliferation of FOXP3-expressing suppressor T cells. *Blood* 2006; **107**: 4417–23.
36 Maher SG, Sheikh F, Scarzello AJ *et al.* IFNalpha and IFN-lambda differ in their antiproliferative effects and duration of JAK/STAT signaling activity. *Cancer Biol Ther* 2008; **7**: 1109–15.
37 Sommereyns C, Paul S, Staeheli P, Michiels T. IFN-lambda (IFN-lambda) is expressed in a tissue-dependent fashion and primarily acts on epithelial cells in vivo. *PLoS Pathog* 2008; **4**: e1000017.
38 Zitzmann K, Brand S, Baehs S *et al.* Novel interferon-lambdas induce antiproliferative effects in neuroendocrine tumor cells. *Biochem Biophys Res Commun* 2006; **344**: 1334–41.
39 Lasfar A, Lewis-Antes A, Smirnov SV *et al.* Characterization of the mouse IFN-lambda ligand-receptor system: IFN-lambdas exhibit antitumor activity against B16 melanoma. *Cancer Res* 2006; **66**: 4468–77.
40 Numasaki M, Tagawa M, Iwata F *et al.* IL-28 elicits antitumor responses against murine fibrosarcoma. *J Immunol* 2007; **178**: 5086–98.
41 Sato A, Ohtsuki M, Hata M, Kobayashi E, Murakami T. Antitumor activity of IFN-lambda in murine tumor models. *J Immunol* 2006; **176**: 7686–94.
42 Wongthida P, Diaz RM, Galivo F *et al.* Type III IFN interleukin-28 mediates the antitumor efficacy of oncolytic virus VSV in immune-competent mouse models of cancer. *Cancer Res* 2010; **70**: 4539–49.
43 Yoshimoto K, Kishida T, Nakano H *et al.* Interleukin-28B acts synergistically with cisplatin tosuppress the growth of head and neck squamous cell carcinoma. *J Immunother* 2011; **34**: 139–48.
44 Bensadoun P, Rodriguez C, Soulier A, Higgs M, Chevaliez S, Pawlotsky JM. Genetic background of hepatocyte cell lines: are in vitro hepatitis C virus research data reliable? *Hepatology* 2011; **54**: 748.
45 Mercer DF, Schiller DE, Elliott JF *et al.* Hepatitis C virus replication in mice with chimeric human livers. *Nat Med* 2001; **7**: 927–33.
46 Tateno C, Yoshizane Y, Saito N *et al.* Near completely humanized liver in mice shows human-type metabolic responses to drugs. *Am J Pathol* 2004; **165**: 901–12.
47 Vanwolleghem T, Libbrecht L, Hansen BE *et al.* Factors determining successful engraftment of hepatocytes and susceptibility to hepatitis B and C virus infection in uPA-SCID mice. *J Hepatol* 2010; **53**: 468–76.
48 Kimura T, Imamura M, Hiraga N *et al.* Establishment of an infectious genotype 1b hepatitis C virus clone in human hepatocyte chimeric mice. *J Gen Virol* 2008; **89**: 2108–13.
49 Hiraga A, Cohen P. Phosphorylation of the glycogen-binding subunit of protein phosphatase-1G by cyclic-AMP-dependent protein kinase promotes translocation of the phosphatase from glycogen to cytosol in rabbit skeletal muscle. *Eur J Biochem* 1986; **161**: 763–9.
50 Suda G, Sakamoto N, Itsui Y *et al.* IL-6-mediated intersubgenotypic variation of interferon sensitivity in hepatitis C virus genotype 2a/2b chimeric clones. *Virology* 2010; **407**: 80–90.
51 Steenbergen RH, Joyce MA, Lund G *et al.* Lipoprotein profiles in SCID/uPA mice transplanted with human hepatocytes become human-like and correlate with HCV infection success. *Am J Physiol Gastrointest Liver Physiol* 2010; **299**: G844–54.
52 Gal-Tanamy M, Keck ZY, Yi M *et al.* In vitro selection of a neutralization-resistant hepatitis C virus escape mutant. *Proc Natl Acad Sci U S A* 2008; **105**: 19450–5.
53 Law M, Maruyama T, Lewis J *et al.* Broadly neutralizing antibodies protect against hepatitis C virus quasispecies challenge. *Nat Med* 2008; **14**: 25–7.
54 Hiraga N, Abe H, Imamura M *et al.* Impact of viral amino acid substitutions and host interleukin-28b polymorphism on replication and susceptibility to interferon of hepatitis C virus. *Hepatology* 2011; **54**: 764–71.
55 Abe H, Ochi H, Maekawa T *et al.* Common variation of IL28 affects gamma-GTP levels and inflammation of the liver in chronically infected hepatitis C virus patients. *J Hepatol* 2010; **53**: 439–43.
56 Urban TJ, Thompson AJ, Bradrick SS *et al.* IL28B genotype is associated with differential expression of intrahepatic interferon-stimulated genes in patients with chronic hepatitis C. *Hepatology* 2010; **52**: 1888–96.
57 Honda M, Sakai A, Yamashita T *et al.* Hepatic ISG expression is associated with genetic variation in interleukin 28B and the outcome of IFN therapy for chronic hepatitis C. *Gastroenterology* 2010; **139**: 499–509.
58 Sarasin-Filipowicz M, Oakeley EJ, Duong FH *et al.* Interferon signaling and treatment outcome in chronic hepatitis C. *Proc Natl Acad Sci U S A* 2008; **105**: 7034–9.
59 Shebl FM, Maeder D, Shao Y, Prokunina-Olsson L, Schadt EE, O'Brien TR. In the absence of HCV infection, interferon stimulated gene expression in liver is not associated with IL28B genotype. *Gastroenterology* 2010; **139**: 1422–4.
60 Lindh M, Lagging M, Norkrans G, Hellstrand K. A model explaining the correlations between IL28B-related genotypes, hepatitis C virus genotypes, and viral RNA levels. *Gastroenterology* 2010; **139**: 1794–6.
61 Taniguchi T, Takaoka A. A weak signal for strong responses: interferon-alpha/beta revisited. *Nat Rev Mol Cell Biol* 2001; **2**: 378–86.
62 Dill MT, Duong FH, Vogt JE *et al.* Interferon-induced gene expression is a stronger predictor of treatment response than IL28B genotype in patients with hepatitis C. *Gastroenterology* 2011; **140**: 1021–31 e10.
63 Asahina Y, Tsuchiya K, Muraoka M *et al.* Association of gene expression involving innate immunity and genetic variation in IL28B with antiviral response. *Hepatology* 2011; **55**: 20–9.
64 Akuta N, Suzuki F, Kawamura Y *et al.* Predictive factors of early and sustained responses to peginterferon plus ribavi-

rin combination therapy in Japanese patients infected with hepatitis C virus genotype 1b: amino acid substitutions in the core region and low-density lipoprotein cholesterol levels. *J Hepatol* 2007; **46**: 403–10.
65 Akuta N, Suzuki F, Sezaki H *et al.* Predictive factors of virological non-response to interferon-ribavirin combination therapy for patients infected with hepatitis C virus of genotype 1b and high viral load. *J Med Virol* 2006; **78**: 83–90.
66 Hayes CN, Kobayashi M, Akuta N *et al.* HCV substitutions and IL28B polymorphisms on outcome of peg-interferon plus ribavirin combination therapy. *Gut* 2011; **60**: 261–7.
67 Tachi Y, Katano Y, Honda T *et al.* Impact of amino acid substitutions in the hepatitis C virus genotype 1b core region on liver steatosis and hepatic oxidative stress in patients with chronic hepatitis C. *Liver Int* 2010; **30**: 554–9.
68 Aly HH, Oshiumi H, Shime H *et al.* Development of mouse hepatocyte lines permissive for hepatitis C virus (HCV). *PLoS ONE* 2011; **6**: e21284.
69 Marcello T, Grakoui A, Barba-Spaeth G *et al.* Interferons alpha and lambda inhibit hepatitis C virus replication with distinct signal transduction and gene regulation kinetics. *Gastroenterology* 2006; **131**: 1887–98.

JOURNAL OF VIRAL HEPATITIS
JVH

Journal of Viral Hepatitis, 2012, **19**, e126–e133 doi:10.1111/j.1365-2893.2011.01516.x

Serum PAI-1 is a novel predictor for response to pegylated interferon-α-2b plus ribavirin therapy in chronic hepatitis C virus infection

D. Miki,[1,2,3] W. Ohishi,[3,4] H. Ochi,[1,2,3] C. N. Hayes,[1,2,3] H. Abe,[1,2,3] M. Tsuge,[3,5] M. Imamura,[2,3] N. Kamatani,[6] Y. Nakamura[7] and K. Chayama[1,2,3]

[1]*Laboratory for Digestive Diseases, Center for Genomic Medicine, RIKEN, Hiroshima, Japan;* [2]*Department of Medicine and Molecular Science, Division of Frontier Medical Science, Programs for Biomedical Research, Graduate School of Biomedical Sciences, Hiroshima University, Hiroshima, Japan;* [3]*Liver Research Project Center, Hiroshima University, Hiroshima, Japan;* [4]*Department of Clinical Studies, Radiation Effects Research Foundation, Hiroshima, Japan;* [5]*Natural Science Center for Basic Research and Development, Hiroshima University, Hiroshima, Japan;* [6]*Center for Genome Medicine, RIKEN, Yokohama, Japan; and* [7]*Laboratory of Molecular Medicine, Human Genome Center, The Institute of Medical Science, University of Tokyo, Tokyo, Japan*

Received April 2011; accepted for publication June 2011

SUMMARY. Obesity and insulin resistance have been reported as negative predictors for sustained virological response (SVR) in hepatitis C virus (HCV) genotype 1 infected patients treated with pegylated interferon-α plus ribavirin. They are also known to affect serum levels of several cytokines including adipocytokines. But the association between these cytokines and treatment outcome has not been fully elucidated. We examined pretreatment serum levels of 14 cytokines among 190 patients who were treated with pegylated interferon-α-2b plus ribavirin for chronic HCV-1b infection with high viral load (≥5 log IU/mL) and analyzed their contribution to treatment response. Plasminogen activator inhibitor-1 (PAI-1), vascular endothelial growth factor, and 11 clinical factors showed significant association with SVR in univariate logistic regression analysis. Four significant factors in multivariate analysis: serum PAI-1 (odds ratio [OR] = 15.42), body mass index (OR = 4.56), rs8099917 (OR = 4.95) and fibrosis stage (OR = 5.18) were identified as independent predictors. We constructed a simple and minimally invasive prediction score for SVR based on the presence of these factors except for fibrosis stage. The accuracy of this score was 73%, and was confirmed using an independent validation cohort consisting of 31 patients (68%). The strongest correlation was between PAI-1 level and platelet count ($r = 0.38$, $P = 1.8 \times 10^{-7}$), and PAI-1 level was inversely correlated with fibrosis stage. Serum PAI-1 is a novel predictor for the response to combination therapy against chronic HCV-1b infection and may be associated with liver fibrosis.

Keywords: adipocytokine, genotype 1b, liver fibrosis, obesity, sustained virological response.

INTRODUCTION

Hepatitis C virus (HCV) is one of the major causes of chronic hepatitis, liver cirrhosis and hepatocellular carcinoma in Japan as well as in most countries [1,2]. The current standard of care is pegylated interferon-α (PEG-IFN-α) and ribavirin (RBV) combination therapy [3]. In spite of recent progress in anti-HCV therapy, still only half of patients infected with genotype 1 show complete eradication. Therefore, it is important to identify reliable predictors for response to combination therapy.

To date, several viral and host factors responsible for sustained virological response (SVR) have been identified. Both HCV genotype and viral load [4] are strong predictors for SVR. The most difficult patients to treat are those having HCV genotype 1 and high viral load, both of which are common in Japan as well as other Eastern countries. Within genotype 1b, amino acid substitutions at positions 70 and 91 of the HCV core protein and multiple substitutions in the interferon sensitivity determining region of the NS5A protein

Abbreviations: AUC, area under the curve; BMI, body mass index; HCV, hepatitis C virus; NPV, negative predictive value; OR, odds ratio; PEG-IFN, pegylated interferon; PPV, positive predictive value; RBV, ribavirin; ROC, receiver operating characteristic; RT-PCR, reverse-transcription polymerase chain reaction; RVR, rapid virological response; SNP, single nucleotide polymorphism; SVR, sustained virological response

Correspondence: Kazuaki Chayama, MD, PhD, Department of Medicine and Molecular Science, Division of Frontier Medical Science, Programs for Biomedical Research Graduate School of Biomedical Sciences, Hiroshima University, 1-2-3 Kasumi, Minami-ku, Hiroshima 734-8551, Japan. E-mail: chayama@hiroshima-u.ac.jp

have also been reported to affect treatment outcome, especially among Japanese patients [5–7]. Host factors responsible for SVR include age [8], gender, degree of hepatic fibrosis [9] and *IL28B* gene variants [10–12]. In addition, obesity and insulin resistance have been reported as independent negative predictors for SVR following combination therapy in chronic hepatitis C patients [13]. On the other hand, it has also been reported that adipocytokines, adipose tissue-derived cytokines, may play an important role in the development of obesity-related insulin resistance [14,15] and that many cytokines including adipocytokines are elevated or decreased in chronic hepatitis C patients. Therefore, it is reasonable to predict that adipocytokines may be associated with outcome of combination therapy, but such associations have yet to be fully investigated. In this study, we aim to elucidate the associations among several cytokines, other clinical data and treatment outcome of combination therapy.

MATERIALS AND METHODS

Study subjects

For the study cohort, data from 190 consecutive patients who were treated between 2005 and 2007 with PEG-IFN-α-2b plus RBV combination therapy for chronic hepatitis C genotype 1b infection with high viral load (≥5 log IU/mL) were collected from Hiroshima University Hospital. Data from 31 patients treated between 2007 and 2008 were also collected as an independent validation cohort using the same criteria. Study subjects tested positive for HCV RNA over a span of more than 6 months and were negative for hepatitis B virus and HIV and showed no evidence for other liver diseases. Patients received weekly injections of PEG-IFN-α-2b at 1.5 μg/kg body weight for 48 weeks, and RBV was administered orally. The amount of RBV was adjusted based on body weight (600 mg for <60 kg, 800 mg for 60–80 kg, and 1000 mg for >80 kg). Patients who received less than 80% of the prescribed dose of both drugs were excluded. Treatment success was evaluated based on SVR, defined as undetectable HCV RNA levels 24 weeks after cessation of treatment. We also defined rapid virological response (RVR) as undetectable HCV RNA at week 4 of treatment. Histopathological diagnosis was made according to the criteria of Desmet *et al.* [16]. All subjects provided written informed consent to participate in the study according to the process approved by the ethical committee of Hiroshima University and RIKEN and conforming to the ethical guidelines of the 1975 Declaration of Helsinki.

HCV RNA levels

HCV RNA levels were measured by reverse-transcription polymerase chain reaction (RT-PCR) using the original Amplicor method, the high range method, or the TaqMan RT-PCR test. The measurement ranges of these assays were 0.5–850 kIU/mL, 5–5000 kIU/mL, and 1.2–7.8 log IU, respectively. Samples exceeding the measurement range were diluted with PBS and reanalyzed. All values are reported as log IU/mL.

SNP genotyping

Single nucleotide polymorphism (SNP) genotyping of rs8099917 was performed using the Invader assay as described previously [17].

Cytokine measurements

Fourteen cytokines, including interleukin (IL) 1β, IL4, IL6, IL10, IL12p70, IL17, IL28a, tumour necrosis factor-α (TNFα), vascular endothelial growth factor (VEGF), adiponectin, total plasminogen activator inhibitor-1 (PAI-1), resistin, leptin and monocyte chemotactic protein-1 (MCP-1) were measured using the multiplex bead array assay on the Luminex Complete System 200 (Luminex Co., Austin, TX, USA) [18,19], with MILLIPLEX™ MAP kits (Millipore, Billerica, MA, USA) and Bio-Plex Pro™ Cytokine Assay kit (Bio-Rad, Benicia, CA, USA) according to the manufacturers' instructions. High Sensitivity Human Cytokine (HSCYTO-60SK) was used for IL 1β, IL4, IL6, IL10, IL12p70, and TNFα, and Human Serum Adipokine Panel A (HADK1-61K-A) was used for adiponectin, total PAI-1, and resistin, Human Serum Adipokine Panel B (HADK2-61K-B) was used for leptin and MCP-1, and Human Cytokine/Chemokine Panel II (MPXHCYP2-62K) was used for IL28a. Bio-Plex Pro Human Cytokine Group I (M50-0KCAF0Y) was used for IL17 and VEGF. All serum samples obtained from patients were stored −80 °C. Less than 60% of the analyzed samples had values above the lower limit of detection for four cytokines (IL4, IL12p70, IL17 and IL28a), so we excluded them from further analysis.

Statistical analysis

All analyses were performed using the R statistical package (http://www.r-project.org). We assessed the normality of continuous data using the Kolmogorov–Smirnov test and found that only total cholesterol had a normal distribution (data not shown), so we used the non-parametric Mann–Whitney *U*-test for all continuous variables despite our relatively large cohort. Chi-squared tests were used for the analysis of categorical data. All statistical analyses were two sided, and $P < 0.05$ was considered significant. Odds ratios (ORs) and 95% confidence intervals were calculated for each factor. Univariate and multivariate logistic regression analyses were used to identify predictors for SVR. Cut-off points for continuous variables were determined by analysis of the receiver operating characteristic (ROC) curve [20] based on the minimum balanced error rate (BER). BER is the average of the proportion of incorrect classification in each class. Variables that achieved statistical significance in univariate

tests were entered into multivariate logistic regression analysis. Patients for whom data was unavailable for one or more of the selected variables were excluded from multivariate analysis. Multivariate logistic regression analysis was performed using stepwise backward elimination based on the AIC score. The chi-squared test was used to compare the accuracy of the prediction score in the study cohort with that of the validation cohort. Correlation coefficients (r) between PAI-1 level and other clinical data were evaluated using Spearman's rank correlation test.

RESULTS

Comparison of characteristics between patients with and without SVR

We compared the characteristics of patients with and without SVR. As shown in Table 1, younger age, higher leukocyte count, higher platelet count, lower gamma-GTP levels, lower fasting blood sugar levels and homozygosity for the rs8099917 major allele (TT) were significantly associated with SVR. Histological findings revealed that lower fibrosis stage and lower activity grade were also associated with SVR. Two cytokines, IL10 and PAI-1, were significantly higher in patients with SVR (P = 0.048 and 0.0034, respectively).

Predictive factors for SVR

In univariate analysis, the following 13 factors were significantly associated with SVR (Table 2): age (<54 years; P = 0.0000138), body mass index (BMI) (<22.2 kg/m^2; P = 0.0135), leukocyte count (≥4440/mm^3; P = 0.00449), platelet count (≥18.1 × 10^4/mm^3; P = 0.000206), alanine aminotransferase (≥68 IU/L; P = 0.00824), gamma-GTP (<38 IU/L; P = 0.00166), triglycerides (≥75 mg/dL; P = 0.0491), fasting blood sugar (<114 mg/dL; P = 0.00379), rs8099917 genotype (TT; P = 0.00068), VEGF (≥79.26 pg/mL; P = 0.00927), PAI-1 (≥25 117.24 pg/mL; P = 0.000157), fibrosis stage (<3; P = 0.0122), and activity grade (<2; P = 0.0364). All nine factors for which the area

Table 1 Comparison of characteristics between patients with and without SVR

	All patients (n = 190)	SVR (n = 74)	Non-SVR (n = 116)	P value
Age (years)†	62 (54–68)	58 (48–66)	64 (57–68)	0.00084*
Gender (M/F)‡	99/91	41/33	58/58	0.47
BMI (kg/m^2)†	22.5 (20.7–25.3)	22.0 (20.6–25.2)	23.1 (20.9–25.2)	0.17
WBC (/mm^3)†	4810 (3960–5940)	5100 (4490–6330)	4585 (3600–5710)	0.014*
Hb (g/dL)†	13.7 (12.6–14.6)	14.0 (13.1–14.7)	13.5 (12.5–14.5)	0.25
Platelet count (×10^4/mm^3)†	14.5 (10.4–18.8)	16.4 (12.5–20.6)	12.7 (9.9–17.4)	0.00035*
ALT (IU/L)†	50 (34–71)	54 (32–84)	50 (37–65)	0.56
Gamma-GT (IU/L)†	39 (25–69)	31 (23–56)	46 (26–77)	0.023*
Total cholesterol (mg/dL)†	170 (150–191)	178 (153–200)	167 (146–185)	0.25
Triglyceride (mg/dL)†	95 (71–150)	99 (77–181)	92 (69–140)	0.20
Fasting blood sugar (mg/dL)†	106 (88–127)	95 (85–112)	110 (92–133)	0.0047*
HbA1c (%)†	5.2 (4.9–5.6)	5.2 (4.9–5.5)	5.2 (4.9–5.6)	0.60
rs8099917 (TT/TG or GG)‡	137/53	64/10	73/43	0.00042*
IL1β (pg/mL)†	0.22 (<LDD–1.15)	0.19 (<LDD–1.13)	0.23 (<LDD–1.10)	0.54
IL6 (pg/mL)†	3.63 (1.79–8.05)	3.29 (1.79–7.77)	3.75 (1.81–8.38)	0.41
IL10 (pg/mL)†	16.58 (10.30–24.67)	18.27 (11.28–28.70)	15.55 (9.73–22.30)	0.048*
TNFα (pg/mL)†	8.96 (5.88–17.93)	8.71 (5.64–17.90)	9.04 (6.25–17.98)	0.87
VEGF (pg/mL)†	104.66 (69.21–156.72)	108.81 (79.38–198.81)	96.46 (65.30–149.49)	0.098
Adiponectin (ng/mL)†	10 841 (7346–16 141)	10 697 (7313–16 066)	11 112 (7346–16 047)	0.73
PAI-1 (pg/mL)†	18 651 (13 830–22 667)	20 302 (15 564–26 746)	17 639 (13 122–21 278)	0.0034*
Resistin (pg/mL)†	14 254 (5058–25 267)	15 025 (6095–27 098)	12 844 (4605–23 251)	0.19
Leptin (pg/mL)†	5026 (2100–9488)	5161 (2100–9670)	4793 (2126–9263)	0.89
MCP-1 (pg/mL)†	284.8 (226.7–373.3)	278.2 (216.7–364.5)	291.9 (231.1–375.4)	0.56
Fibrosis stage (0–1/2/3/4/ND)†	59/55/23/18/35	27/24/8/1/14	32/31/15/17/21	0.015*
Activity grade (0–1/2/3/ND)†	46/85/21/38	24/32/4/14	22/53/17/24	0.0099*

<LDD, less than the lower limit of detection; ND, not determined; BMI, body mass index; WBC, leukocytes; Hb, haemoglobin; ALT, alanine aminotransferase; Gammma-GT, gammma-glutamyl transpeptidase; IL, interleukin; TNF, tumour necrosis factor; VEGF, vascular endothelial growth factor; PAI, plasminogen activator inhibitor; MCP, monocyte chemotactic protein.
For categorical data, the number of patients in each category is shown. For continuous data, the median and 25–75th percentile are displayed. †Mann–Whitney U-test. ‡Chi-square test. *Siginificant at the 0.05 level.

Table 2 Significant predictive factors for SVR using univariate and multivariate logistic regression analysis

		Univariate				Multivariate			
Variable†	ROC_AUC	*n*	OR	95% CI	*P* value	*n*	OR	95% CI	*P* value
Age <54 years	0.64	190	4.86	2.39–9.90	0.0000138*				
Gender: male	0.53	190	1.25	0.70–2.24	0.467				
BMI <22.2 kg/m^2	0.56	190	2.12	1.17–3.82	0.0135*	100	4.56	1.34–15.53	0.0154*
WBC ≥4440/mm^3	0.61	189	2.59	1.35–4.98	0.00449*				
Hb ≥14.0 g/dL	0.55	190	1.61	0.90–2.90	0.114				
Platelet count ≥18.1 × 10^4/mm^3	0.65	190	3.44	1.80–6.61	0.000206*	100	2.87	0.84–9.85	0.0955
ALT ≥68 IU/L	0.53	190	2.37	1.25–4.47	0.00824*				
Gamma-GT <38 IU/L	0.60	189	2.63	1.44–4.81	0.00166*				
Total cholesterol ≥178 mg/dL	0.55	171	1.79	0.96–3.34	0.0708				
Triglyceride ≥75 mg/dL	0.57	138	2.23	1.01–4.93	0.0491*	100	3.37	0.93–12.23	0.0648
Fasting blood sugar <114 mg/dL	0.64	143	3.10	1.45–6.67	0.00379*				
HbA1c <6.4%	0.53	146	2.96	0.81–10.8	0.102				
rs8099917: TT	0.62	190	3.77	1.76–8.11	0.00068*	100	4.95	1.13–21.85	0.0349*
IL1β <1.74 pg/mL	0.53	190	1.58	0.73–3.43	0.254				
IL6 <13.66 pg/mL	0.54	190	2.51	0.96–6.54	0.0606				
IL10 ≥12.84 pg/mL	0.59	190	1.86	1.00–3.45	0.0504				
TNFα <6.03 pg/mL	0.51	190	1.49	0.78–2.86	0.235				
VEGF ≥79.26 pg/mL	0.57	190	2.36	1.24–4.50	0.00927*	100	2.70	0.71–10.23	0.146
Adiponectin <11 076.65 ng/mL	0.51	190	1.46	0.81–2.62	0.21				
PAI-1 ≥25 117.24 pg/mL	0.63	190	4.59	2.09–10.09	0.000157*	100	15.42	3.00–79.18	0.00105*
Resistin ≥21 580.23 pg/mL	0.56	190	1.75	0.94–3.27	0.0819				
Leptin ≥4418.96 pg/mL	0.51	190	1.49	0.82–2.69	0.195				
MCP-1 <186.81 pg/mL	0.52	190	2.01	0.94–4.33	0.0746				
Fibrosis stage <3	0.61	155	2.88	1.26–6.58	0.0122*	100	5.18	1.12–24.11	0.0362*
Activity grade <2	0.61	152	2.13	1.05–4.30	0.0364*				

ROC_AUC, area under the receiver operating characteristic curve; OR, odds ratio; CI, confidence interval.
Variables with a *P* value <0.05 were included in the multivariate model. Variables were selected using stepwise backward selection. †Continuous variables were split into two categories by analysis of the ROC curve. The favourable category for SVR is shown for each variable. *Significant.

under the ROC curve (ROC_AUC) was ≥0.60 were significant in univariate logistic regression analysis. Four out of these 13 factors were independently associated with SVR under multivariate analysis: PAI-1 (P = 0.00105, OR = 15.42), BMI (P = 0.0154, OR = 4.56), rs8099917 (P = 0.0349, OR = 4.95), and fibrosis stage (P = 0.0362, OR = 5.18). Finally, pretreatment serum PAI-1 level, which has not been reported previously, was revealed as the most significant factor for SVR in this study cohort (Table 2).

Prediction score for SVR in the study and validation cohorts

We tried to construct a simple and minimally invasive prediction score for SVR based on these independent predictors except for fibrosis stage. Liver biopsy has long remained the gold standard for staging of fibrosis, but it is an invasive test with potential for serious, albeit rare, complications [21]. Hence, we excluded fibrosis stage from the score. In this scoring method, 1 point each was assigned for PAI-1 (≥25 117.24 pg/mL), BMI (<22.2 kg/m^2), and rs8099917 (TT). Points were summed in each patient, and the combined point value was assigned as the prediction score of the patient. As shown in Table 3, the proportion of patients assigned 1 point was higher in the SVR group than the non-SVR group for each of the three factors. Higher combined scores predicted higher SVR rates, i.e., patients who scored 2 or 3 had a higher SVR rate (63.1%; Fig. 1). In contrast, patients who scored 0 or 1 had a lower SVR rate (19.8%). Based on this threshold, the accuracy of the prediction score for SVR versus non-SVR was 73% (138/190) in this study cohort with ROC_AUC of 0.74. Specificity, sensitivity, and positive predictive value (PPV) and negative predictive value (NPV) for SVR were 73%, 72%, 63% and 80%, respectively.

We next evaluated the accuracy of the prediction score using an independent validation cohort consisting of 31 patients (SVR, 9; non-SVR, 22) and reobserved the same

Table 3 Distributions of combined score assigned to patients in the study cohort and the validation cohort

	Study cohort (n = 190)			Validation cohort (n = 31)		
	SVR	Non-SVR	SVR rate (%)	SVR (n = 9)	Non-SVR (n = 22)	SVR rate (%)
Age (years)	58 (48–66)	64 (57–68)		58 (55–64)	61 (53–68)	
Gender (M/F)	41/33	58/58		5/4	10/12	
BMI (kg/m^2)	22.0 (20.6–25.2)	23.1 (20.9–25.2)		22.6 (21.5–23.8)	23.0 (21.0–24.7)	
score: 1/0 rs8099917	43/31	46/70		4/5	6/16	
score: 1/0	64/10	73/43		6/3	10/12	
PAI-1 (pg/mL)	20 302 (15 564–26 746)	17 639 (13 122–21 278)		25 688 (22 185–30 591)	17 728 (15 422–26 666)	
Score: 1/0	24/50	11/105		5/4	7/15	
Combined score						
0	3	19	13.6	1	6	14.3
1	18	66	21.4	3	10	23.1
2	46	29	61.3	3	5	37.5
3	7	2	77.8	2	1	66.7
0–3	74	116	38.9	9	22	29.0

For categorical data, the number of patients in each category is shown.
For continuous data, the median and 25th–75th percentile are displayed.

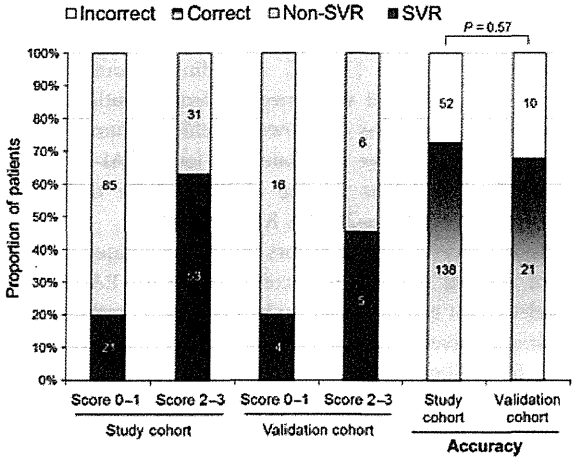

Fig. 1 Associations between combined score and treatment outcome. The accuracy of the prediction score with cut-off of <2 for SVR versus non-SVR in each cohort is also displayed. Number in bar indicates the number of patients. The accuracies of two cohorts are compared using the chi-squared test, and were not significantly different.

tendency in the validation cohort: the proportion of patients assigned 1 point was higher in the SVR group than in the non-SVR group for all three factors, and a higher combined score predicted higher SVR rate (Table 3). As shown in Fig. 1, the SVR rate of patients who scored 2 or 3 was more than twice as high as that of patients who scored 0 or 1 (45.5% and 20.0%, respectively). The accuracy of the prediction score in this validation cohort (21/31, 68%) was slightly reduced compared to that in the study cohort (73%), but the difference was not significant (P = 0.57). In the validation cohort, ROC_AUC was 0.68 and specificity, sensitivity, and PPV and NPV for SVR were 73%, 56%, 46% and 80%, respectively. Specificity and NPV had the same values between the two cohorts, but sensitivity and PPV were reduced in the validation cohort (−16% and −17%, respectively).

Subsequently, we also predicted SVR using RVR, which is well known as an important predictor [22–24]. The data of HCV-negativity at 4 weeks were available in 161 patients. Of 161 patients, only 40 patients (24.8%) showed RVR. Of 40 patients with RVR, 29 patients achieved SVR. As a result, prediction using RVR showed higher PPV and specificity than our score (PPV, 0.73 *vs* 0.63; specificity, 0.89 *vs* 0.73) but conversely, prediction using RVR showed lower NPV and sensitivity (NPV, 0.71 *vs* 0.80; sensitivity, 0.45 *vs* 0.72). Finally, the accuracy of the prediction using RVR was 0.71, which was similar to ours; 0.73 in the study cohort and 0.68 in the validation cohort. In our cohort of Japanese patients infected with HCV-1b with high viral load, overall SVR rate was poor (83/221 = 37.6%) and prediction of SVR was not sufficient even if using RVR. Therefore use of not only a predictor during therapy such as RVR but also a pretreatment predictor such as our score may be useful to predict SVR.

Correlation between PAI-1 level and other clinical data

We examined the correlations between the most significant predictor, PAI-1 level, and all of the other clinical data analyzed in the study cohort. As shown in Table 4, six

Table 4 Spearman correlation between PAI-1 level and other clinical data

	n	*R*	*P* value
Age (years)	190	-0.23	0.0013
Gender (Male)	190	0.20	0.0067
WBC (/mm^3)	189	0.22	0.0028
Platelet count (×10^4/mm^3)	190	0.38	1.8×10^{-7}
Triglyceride (mg/dL)	138	0.24	0.0043
Fibrosis stage (0–1/2/3/4)	155	-0.20	0.012

Only factors with correlation coefficient (r) ≥0.2 or ≤−0.2 are shown.

factors showed significant correlation with PAI-1 level ($r \geq 0.2$ or ≤ -0.2, $P < 0.05$). Platelet count showed the strongest correlation ($r = 0.38$. $P = 1.8 \times 10^{-7}$) and fibrosis stage was inversely correlated (Fig. 2a and b, respectively), suggesting the close association between PAI-1 and liver fibrosis. Age was also inversely correlated ($r = -0.23$) and, in addition, male gender, leukocyte count, and triglycerides were significantly correlated with PAI-1 level.

DISCUSSION

In this study, we found that pretreatment serum PAI-1 level was a novel independent predictive marker for the response to PEG-IFN-α-2b plus RBV therapy in patients with hepatitis C, which has not been reported before. We propose a simple and noninvasive prediction score for SVR consisting of rs8099917, BMI and PAI-1 level. The accuracy of this score was confirmed using an independent validation cohort. We also found that serum PAI-1 level was correlated with a number of other clinical factors such as platelet count, fibrosis stage, age, gender, leukocyte count and triglyceride level.

PAI-1 is the primary physiological inhibitor of tissue-type plasminogen activator and urokinase-like plasminogen activator and inhibits both fibrinolysis and proteolysis [25]. Circulating PAI-1 levels in humans are increased in obesity and the insulin resistance syndrome [14]. Adipose tissue produces and secretes a large number of hormones, cytokines, and proteins that affect glucose homeostasis and insulin sensitivity, including tumour necrosis factor-alpha, PAI-1, leptin, resistin, and adiponectin [14,15]. Among the adipocytokines that we examined, PAI-1 was identified as an independent predictor for SVR, but the mechanism by which PAI-1 affects treatment outcome of combination therapy for chronic hepatitis C patients is unclear.

One possible mechanism is suggested by an interesting report postulating that PAI-1 activates the Janus kinase (Jak)-signal transducer and activator of transcription (STAT) signalling system and that this activation is mediated by the low density lipoprotein receptor-related protein [26]. IFNs are known to activate the Jak-STAT signalling system and induce the transcription of IFN-stimulated genes (ISGs), which are essential for the induction of an antiviral state [27,28]. Based on these findings, PAI-1 may affect SVR via this signalling pathway through activation in a similar way to IFNs. However, other reports demonstrate that up-regulation of ISGs in the liver prior to treatment confers a poor treatment outcome [29,30].

On the other hand, PAI-1 level was correlated with both age and gender in our study. It was reported that response to combination therapy is poorer in older female patients with hepatitis C in Japan [31,32]. According to our findings (Table 4), PAI-1 level was lower in female patients than male patients and was also lower in elderly than younger patients. Therefore, we speculate that lower PAI-1 level in elderly females might be one of reasons for their poor response to PEG-IFN-α-2b plus RBV therapy.

Among several clinical factors that we examined, platelet count showed the strongest correlation with PAI-1 level. Platelet count is well known to be inversely correlated with the stage of liver fibrosis in patients with chronic hepatitis C [33]. In addition, we also observed an inverse correlation between PAI-1 level and fibrosis stage. PAI-1 assumed to positively correlate with fibrosis due to its inhibitive effect on fibrinolysis, but actually we found the opposite result. Some

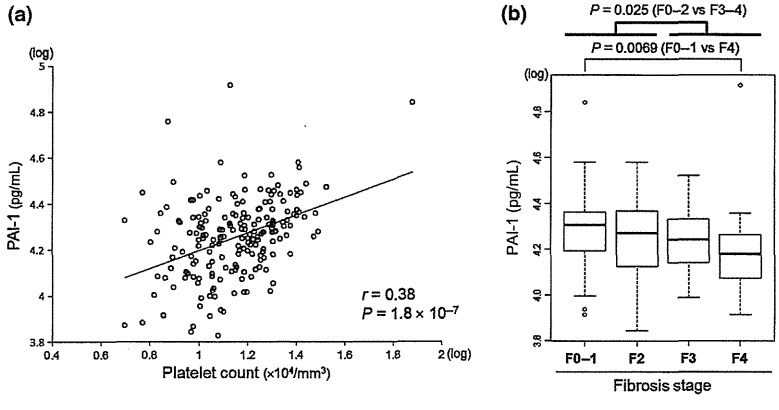

Fig. 2 The correlations between PAI-1 level and platelet count as well as fibrosis stage. (a) PAI-1 level and platelet count are significantly correlated using Spearman's tests. The solid line represents a least squares best fit line. (b) PAI-1 level is inversely correlated with fibrosis stage. The box indicates the inter-quartile range (25% and 75%) and the line within the box represents the median. *P* values were calculated by Mann–Whitney *U*-test.

reports suggest a positive correlation between PAI-1 and hepatic fibrosis using animal models, such as the bile duct ligation model [34,35], but recently von Montfort *et al.* reported that PAI-1 plays a protective role in hepatic fibrosis using another, more severe, model of hepatic fibrosis caused by carbon tetrachloride (CCl_4) [36]. They showed that hepatic mRNA expression of collagen Iα1 was elevated in PAI-1-deficient mice after CCl_4 exposure and also that livers from PAI-1-deficient mice have an impaired regenerative response to injury, in part via a mechanism involving impaired hepatocyte growth factor (HGF) maturation or via impaired HGF signalling via p38 phosphorylation. The role of PAI-1 in hepatic fibrosis is still controversial, but here we suggest a clinically protective role of PAI-1.

In this study, we identified pretreatment serum PAI-1 level as an independent predictor for SVR and suggest a scoring method for predicting outcome of combination therapy. Interestingly, this prediction score consists of one SNP and two factors that are strongly associated with metabolic syndrome. In addition to lower BMI and higher PAI-1 level, higher triglyceride and lower fasting blood sugar were associated with SVR in univariate analysis (Table 2), and PAI-1 level is correlated with triglyceride level (Table 4). These results suggest that metabolic factors have strong effects and close connections to treatment outcome in HCV patients. It may be worth investigating whether intervention in such metabolic disorders improves treatment outcome. In the near future, direct-acting antiviral agents such as protease inhibitors will become available [37,38]. As such drugs are very powerful, the predictive ability of PAI-1 might become less significant. However, PEG-IFN plus RBV combination therapy will still be used to treat non-genotype 1b infected patients. Accordingly, the predictive value of PAI-1 should be assessed in such patients. Functional studies using animal models have suggested a role for PAI-1 in liver fibrosis [34–36], and should be investigated further with regard to therapy.

In conclusion, measurement of pretreatment PAI-1 level as well as rs8099917 genotype could be useful in planning an individualized treatment strategy against HCV.

ACKNOWLEDGEMENTS

The authors thank Yasufumi Hayashida, Takako Yokogi, Kana Izumoto, and Takeshi Kishi for the excellent technical assistance, and Junko Sakamiya and Aya Furukawa for clerical assistance. This study was supported in part by a Grant-in-Aid for Scientific Research from the Japanese Ministry of Labor, Health and Welfare.

DISCLOSURES

The authors who have taken part in this study declared that they do not have anything to disclose regarding conflict of interest with respect to this manuscript.

REFERENCES

1 Yang JD, Roberts LR. Hepatocellular carcinoma: a global view. *Nat Rev Gastroenterol Hepatol* 2010; 7: 448–458.
2 Ikeda K, Saitoh S, Suzuki Y, *et al.* Disease progression and hepatocellular carcinogenesis in patients with chronic viral hepatitis: a prospective observation of 2215 patients. *J Hepatol* 1998; 28: 930–938.
3 Manns MP, McHutchison JG, Gordon SC, *et al.* Peginterferon alfa-2b plus ribavirin compared with interferon alfa-2b plus ribavirin for initial treatment of chronic hepatitis C: a randomised trial. *Lancet* 2001; 358: 958–965.
4 Ghany MG, Strader DB, Thomas DL, Seeff LB. Diagnosis, management, and treatment of Hepatitis C: an update. *Hepatology* 2009; 49: 1335–1374.
5 Enomoto N, Sakuma I, Asahina Y, *et al.* Comparison of full-length sequences of interferon-sensitive and resistant hepatitis C virus 1b. Sensitivity to interferon is conferred by amino-acid substitutions in the NS5A region. *J Clin Invest* 1995; 96: 224–230.
6 Akuta N, Suzuki F, Kawamura Y, *et al.* Predictive factors of early and sustained responses to peginterferon plus ribavirin combination therapy in Japanese patients infected with hepatitis C virus genotype 1b: amino acid substitutions in the core region and low-density lipoprotein cholesterol levels. *J Hepatol* 2007; 46: 403–410.
7 Hayes CN, Kobayashi M, Akuta N, *et al.* HCV substitutions and IL28B polymorphisms on outcome of peginterferon plus ribavirin combination therapy. *Gut* 2011; 60: 261–267.
8 Iwasaki Y, Ikeda H, Araki Y, *et al.* Limitation of combination therapy of interferon and ribavirin for older patients with chronic hepatitis C. *Hepatology* 2006; 43: 54–63.
9 Everson GT, Hoefs JC, Seeff LB, *et al.* Impact of disease severity on outcome of antiviral therapy for chronic hepatitis C: lessons from the HALT-C trial. *Hepatology* 2006; 44: 1675–1684.
10 Ge D, Fellay J, Thompson AJ, *et al.* Genetic variation in IL28B predicts hepatitis C treatment-induced viral clearance. *Nature* 2009; 461: 399–401.
11 Suppiah V, Moldovan M, Ahlenstiel G, *et al.* IL28B is associated with response to chronic hepatitis C interferon-alpha and ribavirin therapy. *Nat Genet* 2009; 41: 1100–1104.
12 Tanaka Y, Nishida N, Sugiyama M, *et al.* Genome-wide association of IL28B with response to pegylated interferon-alpha and ribavirin therapy for chronic hepatitis C. *Nat Genet* 2009; 41: 1105–1109.
13 Romero-Gómez M, Del Mar Viloria M, Andrade RJ, *et al.* Insulin resistance impairs sustained response rate to peginterferon plus ribavirin in chronic hepatitis C

patients. *Gastroenterology* 2005; 128: 636–641.
14 Pittas AG, Joseph NA, Greenberg AS. Adipocytokines and insulin resistance. *J Clin Endocrinol Metab* 2004; 89: 447–452.
15 Ahima RS, Flier JS. Adipose tissue as an endocrine organ. *Trends Endocrinol Metab* 2000; 11: 327–332.
16 Desmet VJ, Gerber M, Hoofnagle JH, Manns M, Scheuer PJ. Classification of chronic hepatitis: diagnosis, grading and staging. *Hepatology* 1994; 19: 1513–1520.
17 Ohnishi Y, Tanaka T, Ozaki K, Yamada R, Suzuki H, Nakamura Y. A high-throughput SNP typing system for genome-wide association studies. *J Hum Genet* 2001; 46: 471–477.
18 Lee SA, Kallianpur A, Xiang YB, *et al.* Intra-individual variation of plasma adipokine levels and utility of single measurement of these biomarkers in population-based studies. *Cancer Epidemiol Biomarkers Prev* 2007; 16: 2464–2470.
19 Gu Y, Zeleniuch-Jacquotte A, Linkov F, *et al.* Reproducibility of serum cytokines and growth factors. *Cytokine* 2009; 45: 44–49.
20 Fawcett T. An introduction to ROC analysis. *Pattern Recogn Lett* 2006; 27: 861–874.
21 Manning DS, Afdhal NH. *Gastroentrerology* 2008; 134: 1670–1681.
22 Davis GL, Wong JB, McHutchison JG, Manns MP, Harvey J, Albrecht J. Early virologic response to treatment with peginterferon alfa-2b plus ribavirin in patients with chronic hepatitis C. *Hepatology* 2003; 38: 645–652.
23 Jensen DM, Morgan TR, Marcellin P, *et al.* Early identification of HCV genotype 1 patients responding to 24 weeks peginterferon α-2a (40 kD)/ribavirin therapy. *Hepatology* 2006; 43: 954–960.
24 Cheng WS, Roberts SK, McCaughan G, *et al.* Low virological response and high relapse rates in hepatitis C genotype 1 patients with advanced fibrosis despite adequate therapeutic dosing. *J Hepatol* 2010; 53: 616–623.
25 Ma LJ, Fogo AB. PAI-1 and kidney fibrosis. *Front Biosci* 2009; 14: 2028–2041.
26 Degryse B, Neels JG, Czekay RP, Aertgeerts K, Kamikubo Y, Loskutoff DJ. The low density lipoprotein receptor-related protein is a motogenic receptor for plasminogen activator inhibitor-1. *J Biol Chem* 2004; 279: 22595–22604.
27 Darnell Jr JE, Kerr IM, Stark GR. Jak-STAT pathways and transcriptional activation in response to IFNs and other extracellular signaling proteins. *Science* 1994; 264: 1415–1421.
28 Blindenbacher A, Duong FH, Hunziker L, *et al.* Expression of hepatitis C virus proteins inhibits interferon alpha signaling in the liver of transgenic mice. *Gastroenterology* 2003; 124: 1465–1475.
29 Feld JJ, Nanda S, Huang Y, *et al.* Hepatic gene expression during treatment with peginterferon and ribavirin: identifying molecular pathways for treatment response. *Hepatology* 2007; 46: 1548–1563.
30 Chen L, Borozan I, Feld J, *et al.* Hepatic gene expression discriminates responders and nonresponders in treatment of chronic hepatitis C viral infection. *Gastroenterology* 2005; 128: 1437–1444.
31 Sezaki H, Suzuki F, Kawamura Y, *et al.* Poor response to pegylated interferon and ribavirin in older women infected with hepatitis C virus of genotype 1b in high viral loads. *Dig Dis Sci* 2009; 54: 1317–1324.
32 Chayama K, Hayes CN, Yoshioka K, *et al.* Accumulation of refractory factors for pegylated interferon plus ribavirin therapy in older female patients with chronic hepatitis C. *Hepatol Res* 2010; 40: 1155–1167.
33 Wai CT, Greenson JK, Fontana RJ, *et al.* A simple noninvasive index can predict both significant fibrosis and cirrhosis in patients with chronic hepatitis C. *Hepatology* 2003; 38: 518–526.
34 Bergheim I, Guo L, Davis MA, Duveau I, Arteel GE. Critical role of plasminogen activator inhibitor-1 in cholestatic liver injury and fibrosis. *J Pharmacol Exp Ther* 2006; 316: 592–600.
35 Zhang LP, Takahara T, Yata Y, *et al.* Increased expression of plasminogen activator and plasminogen activator inhibitor during liver fibrogenesis of rats: role of stellate cells. *J Hepatol* 1999; 31: 703–711.
36 von Montfort C, Beier JI, Kaiser JP, *et al.* PAI-1 plays a protective role in CCl_4-induced hepatic fibrosis in mice: role of hepatocyte division. *Am J Physiol Gastrointest Liver Physiol* 2010; 298: G657–G666.
37 Sarrazin C, Zeuzem S. Resistance to direct antiviral agents in patients with hepatitis C virus infection. *Gastroenterology* 2010; 138: 447–462.
38 Pawlotsky JM. Treatment failure and resistance with direct-acting antiviral drugs against hepatitis C virus. *Hepatology* 2011; 53: 1742–1751.

Dig Dis Sci
DOI 10.1007/s10620-012-2514-8

ORIGINAL ARTICLE

Cytoglobin May Be Involved in the Healing Process of Gastric Mucosal Injuries in the Late Phase Without Angiogenesis

Fumio Tanaka · Kazunari Tominaga · Eiji Sasaki · Mitsue Sogawa · Hirokazu Yamagami · Tetsuya Tanigawa · Masatsugu Shiba · Kenji Watanabe · Toshio Watanabe · Yasuhiro Fujiwara · Norifumi Kawada · Katsutoshi Yoshizato · Tetsuo Arakawa

Received: 30 July 2012 / Accepted: 3 December 2012

Abstract
Background and Aims Cytoglobin (Cygb) is the newest globin family and is upregulated during hypoxia to maintain the oxygen status. Herein, we investigated Cygb expression in both acute and chronic gastric mucosal injuries.
Methods Acute gastric mucosal injuries in rats were produced by oral administration of indomethacin, followed by sacrifice at 1, 3, 6, 24, and 48 h. Gastric ulcer was produced by acetic acid, followed by sacrifice on days 3, 7, 11, 18, and 25. Each protein expression of Cygb and hypoxia-inducible factor (HIF)-1α was evaluated by western blotting. We measured vascular endothelial growth factor (VEGF) mRNA by RT-PCR and examined localization of Cygb by immunofluorescence.
Results In indomethacin-induced injury, Cygb protein was significantly increased at 24 h. In ulcerated tissues, HIF-1α protein was significantly increased on days 7 and 11 (1.83 ± 0.11 and 2.12 ± 0.19 folds, respectively, $p < 0.05$ and 0.01), which corresponded to the early healing phase. In contrast, Cygb protein was significantly increased on days 11 and 18 (1.87 ± 0.13 and 1.60 ± 0.06 folds, respectively, $p < 0.05$), which demonstrated late phase. Though these proteins peaked on day 11, VEGF mRNA was gradually increased from day 11 to 18. Cygb was expressed in fibroblasts and myofibroblasts in both acute and chronic models. Cygb and HIF-1α were abundantly colocalized at the ulcer margin before angiogenesis development. However, faint localization was observed with angiogenesis.
Conclusions Cygb may be involved in the healing process of gastric mucosal injuries in the late phase without angiogenesis.

Keywords Stomach ulcer · Hypoxia · Angiogenesis · Mesenchyme · Fibroblast

Abbreviations

Cygb	Cytoglobin
NO	Nitric oxide
HRE	Hypoxia response element
HIF	Hypoxia-inducible factor
VEGF	Vascular endothelial growth factor
RT-PCR	Reverse transcription-polymerase chain reaction
α-SMA	α-smooth muscle actin
vWF	von Willebrand factor

Introduction

Cytoglobin (Cygb), a globin similar to myoglobin, was discovered by the proteomics approach of rat hepatic stellate cells in 2001 [1]. The expression of Cygb was

F. Tanaka · K. Tominaga (✉) · M. Sogawa · H. Yamagami · T. Tanigawa · M. Shiba · K. Watanabe · T. Watanabe · Y. Fujiwara · T. Arakawa
Department of Gastroenterology, Graduate School of Medicine, Osaka City University, 1-4-3 Asahimachi, Abeno-ku, Osaka 545-8585, Japan
e-mail: tomy@med.osaka-cu.ac.jp

E. Sasaki
Department of Gastroenterology, Osaka City General Hospital, Osaka, Japan

N. Kawada
Department of Hepatology, Graduate School of Medicine, Osaka City University, Osaka, Japan

K. Yoshizato
PhoenixBio Co, Ltd, Hiroshima, Japan

Published online: 10 January 2013

detected in normal rat and human tissues such as brain, heart, kidney, lung, liver, stomach, intestine, trachea, and liver [2]. Immunohistochemistry and immunoelectron microscopy revealed that Cygb was localized in fibroblast-like cells in splanchnic organs, namely, the vitamin A-storing cell lineage; however, Cygb was not localized in epithelial cells, endothelial cells, muscle cells, blood cells, macrophages, or dermal fibroblasts [3]. Cygb plays a potential protective role against hypoxia. It functions as a scavenger of nitric oxide (NO) or reactive oxygen species and as an oxygen transporter and sensor [4–6]. Cygb functions as an intracellular oxygen transporter because this protein has 40 % amino acid sequence homology with myoglobin [7]. Cygb may act as a protein supplying oxygen to O_2-requiring cellular reactions unrelated to mitochondrial respiration [6]. In addition, it exhibits dioxygenase enzymatic activity and plays a role in fibrotic organ disorder [3, 8].

Cygb expression is upregulated under hypoxic conditions in vitro and in vivo [9, 10]. Upregulation of Cygb mRNA upon exposure to a hypoxic condition is observed in mouse and rat brain, skeletal muscle, liver, and heart. Analysis of the human Cygb promoter region revealed the presence of hypoxia response element (HRE) in the 5′ UTR region of the *CYGB* gene, which suggested that it might have an oxygen-dependent regulation. Several lines of evidence suggested that Cygb was hypoxia-inducible [4, 10]. A previous study showed that the binding of hypoxia-inducible factor-1 (HIF-1) protein to HRE motifs directly induced the promotion of Cygb transcription under hypoxic conditions in vitro [11].

Ischemia and tissue hypoxia induce vasodilatation and angiogenesis to maintain blood flow. Many vasoactive substances and angiogenic factors, such as vascular endothelial growth factor (VEGF), are expressed in response to hypoxia to induce angiogenesis. VEGF, an endothelial cell-specific mitogen, is the most potent angiogenic growth factor [12]. VEGF has been implicated in the angiogenic response to gastric ulceration and ethanol-induced gastric erosions [13, 14]. Hypoxia induces VEGF expression via HIF-1 which is a transcription factor composed of two subunits: HIF-1α and HIF-1β [15, 16]. Under normoxic conditions, the HIF-1β protein is relatively stable, whereas the HIF-1α protein is continuously produced and rapidly degraded. In contrast, hypoxia stabilizes the HIF-1α protein leading to its accumulation within the cell and formation of active HIF-1 complex [17]. HIF-1α is the key factor that induces angiogenesis during the healing of gastric ulcer, nonsteroidal anti-inflammatory drug-induced gastric mucosal lesion, and esophageal ulcer [18, 19]. In addition, HIF-1 is recognized as the master regulator of the cellular hypoxia responses [20]. A recent study demonstrated that the expression of Cygb was altered in HIF knockout mice, supporting an important role for HIF in Cygb expression [4, 11].

Healing of gastric ulcers involves many vasoactive substances and angiogenic factors, including endothelin, NO, and VEGF [13]. These factors are known to be induced by HIF-1α that was highly expressed during the early phase of gastric ulcer healing [15]. However, the pathophysiological role of Cygb in mucosal injury of the stomach has remained to be elucidated. The aim of this study was to investigate Cygb expression and its possible involvement in the repair process of gastric mucosal injuries in rat.

Materials and Methods

Animals

All experimental procedures were approved by the Animal Care Committee of Osaka City University Graduate School of Medicine. In this study, we used 8-week-old male Wistar rats (purchased from Clea Japan, Osaka, Japan) weighing about 200 g. The animals were given standard rat chow diet (CE-2; Clea Japan) and water ad libitum.

Production of Acute Gastric Mucosal Injury

Rats were starved for 24 h before the experiment as follows; acute gastric injury was induced by oral administration of indomethacin or HCl-EtOH according to the method described in a previous report ($N = 3$) [21, 22]. Indomethacin was suspended in 0.5 % methyl cellulose and administered at a dose of 20 mg/kg. Rats were administered 0.15 N HCl in 60 % EtOH (0.5 mL/100 g).

Production of Experimental Gastric Ulcer

Experimental gastric ulcers were produced in rats according to the method described in a previous report [23, 24]. In brief, rats were fasted for 12 h and laparotomy was performed under ether anesthesia. A round plastic mold (6 mm in diameter) was placed tightly on the anterior serosal surface of the antral-oxyntic border. Acetic acid (100 %, 0.06 mL) was poured into the mold and allowed to remain on the gastric wall for 60 s ($N = 5$–6). In control rats, laparotomy was performed under ether anesthesia and their abdomens were closed without the above treatment (sham-operated rats, $N = 5$–6).

Experimental Protocol

In acute gastric injury models, rats were killed by cervical dislocation at the following time after drug administration:

1, 3, 6, 24, and 48 h in the indomethacin model, and 0.5, 2, 6, and 24 h in the HCl-EtOH model. For histological study, rats were killed at 48 h in the indomethacin model. Stomachs were rapidly excised and opened along the greater curvature. Tissues were rinsed in saline and the extent of gastric damage was evaluated by calculating the total length of the macroscopically visible erosions. Gastric tissues were cut to a size of 5 × 5 mm for western blotting and 5 × 10 mm for immunofluorescence. These tissues were frozen in liquid nitrogen and stored at −80 °C until the assay.

In the experimental gastric ulcer model, rats were killed on days 3, 7, 11, 18, or 25 after gastric ulcer formation, and the ulcerated gastric tissues (total gastric walls including ulcerated area, weighing 100–120 mg) were rapidly removed. As control tissues, intact gastric tissues (in the same region as ulcerated tissues) were rapidly excised from sham-operated rats. These tissues were rinsed in saline, frozen in liquid nitrogen, and stored at −80 °C until protein assay was performed. For quantitative real-time reverse transcription-polymerase chain reaction (RT-PCR), rats were killed on days 11 and 18, and their stomachs were removed and processed as described below. For histological study, the rats were killed on day 11.

Western Blot Analysis

Expression of Cygb and HIF-1α proteins were examined by western blotting. Gastric tissues were homogenized and lysed on ice in buffer containing 0.5 % Nonident P-40, 40 mM Tris–HCl (pH 8.0), 120 mM NaCl, 1 mM phenylmethylsulfonyl fluoride (PMSF), and 10 μg of leupeptin per milliliter. The protein content of the lysate was measured with a modified bicinchoninic acid method (BCA) protein assay reagent kit (Pierce, IL, USA). Proteins were denatured with sodium dodecyl sulfate (SDS) sample buffer and subjected to 10 % SDS–polyacrylamide gel electrophoresis (PAGE) and transferred to a polyvinylidene difluoride membrane. Membranes were blocked in TBS buffer [10 mM Tris–HCl (pH 7.5), 100 mM NaCl, 0.1 % Tween-20] containing 5 % bovine serum albumin (BSA), and then incubated with the specific polyclonal antibody against Cygb (diluted 1:1,000) or monoclonal antibody against HIF-1α (1:500) overnight. The bound antigen–antibody complexes were detected with anti-rabbit IgG-horseradish peroxidase (HRP) by using enhanced chemiluminescence in accordance with the manufacturer's instructions (Amersham, IL, USA). Relative expressions were represented as percentages of sham-operated rats (controls).

Quantitative Real-Time RT-PCR

We measured mRNA expression of HIF-1α and VEGF in the ulcerated gastric tissues by quantitative real-time RT-PCR. Real-time RT-PCR analyses were performed by using the previously described protocol [25]. Glyceraldehyde-3-phosphate dehydrogenase (GAPDH) was used as an internal standard with Taqman GAPDH control reagents (PE Applied Biosystems). The mean value in the sham-operated tissues (controls) was taken as 1.

Antibodies

Rabbit polyclonal IgG antibodies against rat Cygb were produced by using a synthetic NH_2-terminal polypeptide of rat Cygb, namely, NH_2-MEKVPGDMEIERRERNEE + Cys-COOH, as an immunogen as described previously [1]. Other antibodies used for immunohistochemistry were as follows: vimentin was detected with mouse monoclonal antibody (Abcam, Tokyo, Japan), α-smooth muscle actin (α-SMA) with mouse monoclonal antibody (Sigma-Aldrich, MO, USA), cytokeratin with mouse monoclonal antibody (Abcam), HIF-1α with mouse monoclonal antibody (Santa Cruz Biotechnology, CA, USA), and von Willebrand factor (vWF) with mouse monoclonal antibody (Santa Cruz). Cygb immunoreactivity was detected using an Alexa Fluor 488-conjugated secondary antibody (Alexa Fluor 488 donkey anti-rabbit, Molecular Probes Inc., OR, USA). Others were detected using an Alexa Fluor 594-conjugated secondary antibody (Alexa Fluor 594 donkey anti-mouse, Molecular Probes). Nuclei were counterstained with DAPI (ProLong Gold antifade reagents with DAPI, Molecular Probes).

Indirect Immunofluorescence

Excised and cut stomachs were embedded in Tissue-Tek® OCT compound (Sakura Finetechnical Co., Ltd., Tokyo, Japan) and then frozen in dry ice. Tissues were cut to 6-μm cryostat sections and mounted on silane-coated glass slides and air dried. And then, the samples were fixed with acetone for 7 min. The sections were incubated with 5 % donkey serum in phosphate-buffered saline (PBS) for 60 min to reduce nonspecific antibody binding and incubated with the specific first antibodies overnight at 4 °C. All antibodies were diluted to 1:250 in Dako antibody diluent with background reducing components (Dako, Tokyo, Japan). After washing with PBS, the sections were incubated with secondary antibodies for 60 min at room temperature. After washing with PBS, sections were mounted using ProLong Gold antifade reagents with DAPI. Tissues were examined with a fluorescent microscope (Olympus BX50, Tokyo, Japan).

Statistical Analysis

Significant differences were assessed by one-way analysis of variance (ANOVA) with Tukey–Kramer post hoc test.

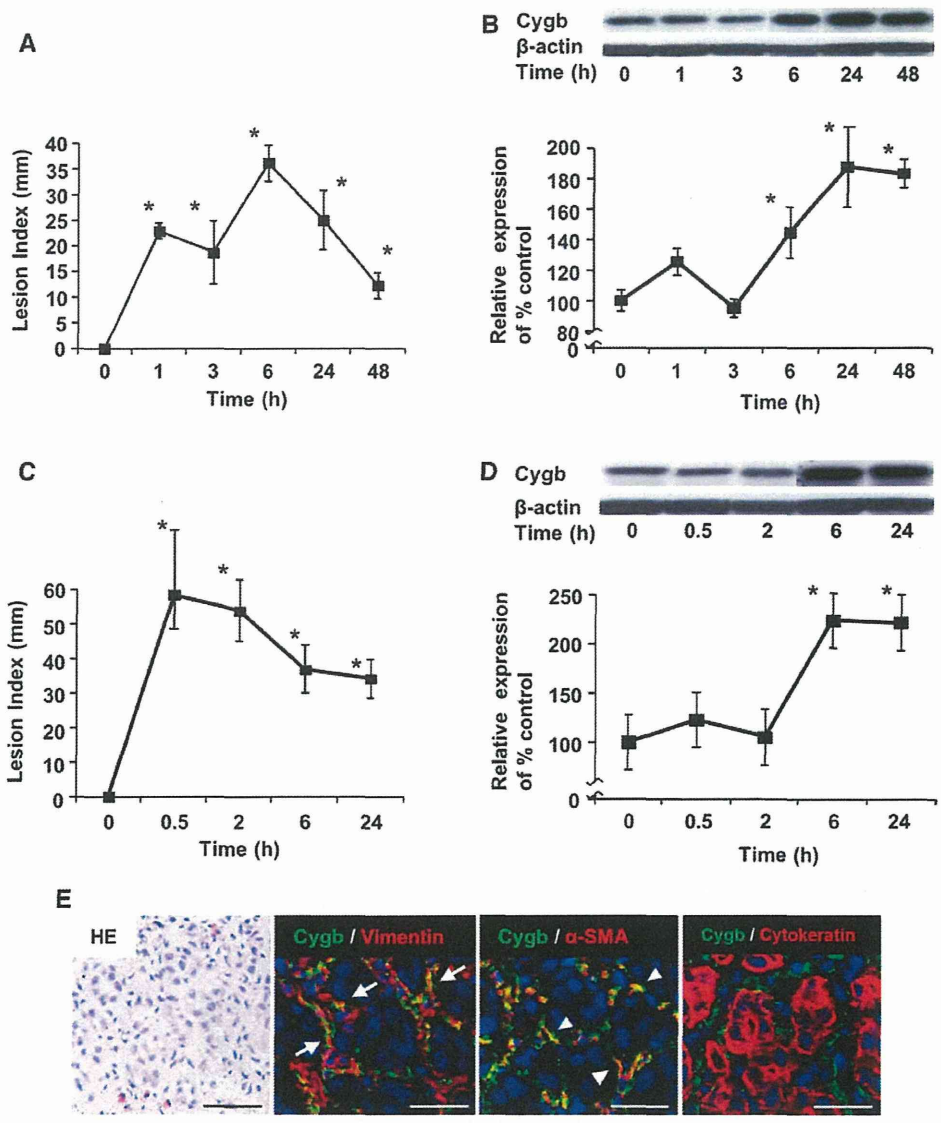

Fig. 1 Cygb protein expression in acute gastric injury models. Lesion index (**a**) and expression of Cygb protein (**b**) in indomethacin-induced gastric mucosal injury. Lesion index (**c**) and expression of Cygb protein (**d**) in HCl-EtOH-induced gastric mucosal injury. Each value represents the mean ± SEM ($N = 3$). *$p < 0.05$ versus control. **e** Localization of Cygb at 48 h after the production of indomethacin-induced acute gastric mucosal injury. The mucosal layer was slightly edematous and the structure of gland was distorted (*first panel* from *left*). Colocalization was observed in the spindle-shaped or linear-shaped cells surrounding the glands, which were indicated to be fibroblasts or myofibroblasts (*second panel, arrow*). Colocalization of Cygb and α-SMA was also observed in the linear-shaped cells, which confirmed the cells were myofibroblasts (*third panel, arrowheads*). Cygb was not expressed in the epithelial cells which were immunoreactive for cytokeratin (*fourth panel*). *HE* hematoxylin and eosin. *Scale bars* 50 μm

Values are expressed as mean ± standard error of mean (SEM). Probability values of less than 0.05 were considered to indicate statistical significance.

Results

Expression of Cygb in Acute Gastric Mucosal Injury Model

In an indomethacin-induced acute injury model, expression of the Cygb protein was increased at 6 h when the lesion index was maximum, and it peaked at 24 h (1.87 ± 0.26 fold, $p < 0.05$ vs. control group; Fig. 1a, b). In the HCl-EtOH model, maximal expression of Cygb protein was observed from 6 to 24 h, while mucosal injury peaked at 0.5 h after HCl-EtOH administration (Fig. 1c, d). These results showed that the level of Cygb protein was increased in the late phase of mucosal healing.

Localization of Cygb in Acute Gastric Mucosal Injury Model

At 48 h after the production of indomethacin-induced acute gastric mucosal injury, Cygb protein expression was still high (Fig. 1b). At the same time, gastric mucosa was quite recovered from erosion and the lesion index was low (Fig. 1a). The mucosal layer was slightly edematous and the structure of gland was distorted (Fig. 1e, first panel from left). Cygb and vimentin were colocalized in the cytoplasm of mesenchymal cells surrounding the glands (second panel). Colocalization was observed in the

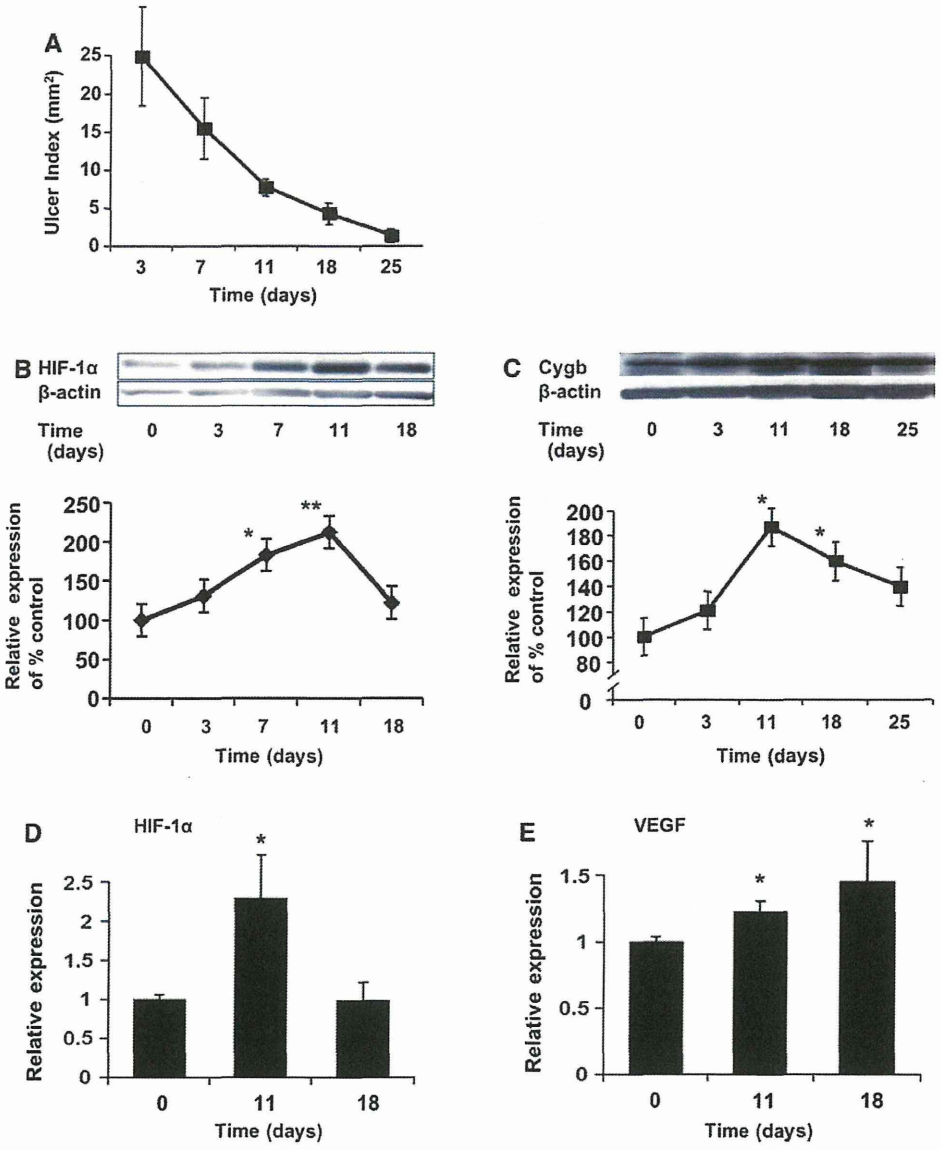

Fig. 2 HIF-1α and Cygb protein expression in an experimental gastric ulcer model. Changes in gastric ulcer size (**a**), expression of HIF-1α protein (**b**), and Cygb protein (**c**) in the ulcerated tissues. HIF-1α protein was significantly increased on day 7 after the production of gastric ulcer (1.83 ± 0.11 folds, $p < 0.05$ vs. control) and sustained up to day 11 (2.12 ± 0.19 folds, $p < 0.01$), which corresponded to the early phase of healing stage. In contrast, Cygb protein was significantly increased on days 11 and 18 (1.87 ± 0.13 and 1.60 ± 0.06 folds, respectively, $p < 0.05$), which corresponded to the late phase of healing. Interestingly, HIF-1α was not significantly increased on day 18 whereas Cygb was increased. There was a difference between HIF-1α and Cygb protein expression in the time phase. Each value represents the mean ± SEM ($N = 5$–6). $^{*}p < 0.05$ and $^{**}p < 0.01$ versus control. mRNA expressions of HIF-1α (**d**) and VEGF (**e**) in the ulcerated gastric tissues. Expression of HIF-1α peaked on day 11. In contrast, VEGF expression was gradually increased from day 11 to 18. VEGF expression peaked at day 18. Each value represents the mean ± SEM ($N = 3$–4). $^{*}p < 0.05$ versus control

spindle-shaped or linear-shaped cells, which were indicated to be fibroblasts or myofibroblasts. Colocalization of Cygb and α-SMA was also observed in the linear-shaped cells, which confirmed the cells were myofibroblasts (third panel). Cygb was not expressed in the epithelial cells which were immunoreactive for cytokeratin (fourth panel).

Expression of HIF-1α and Cygb Protein in the Ulcerated Gastric Tissues

The sizes of gastric ulcer induced by acetic acid was 24.9 ± 2.9, 15.2 ± 2.7, 7.8 ± 0.5, 4.4 ± 0.6, and 1.4 ± 0.4 mm^2 on days 3, 7, 11, 18, and 25, respectively (Fig. 2a). These results were consistent with previous macroscopic and microscopic findings [24, 26]. Expression of HIF-1α protein in the ulcerated gastric tissues was significantly increased on day 7 after the production of gastric ulcer (1.83 ± 0.11 folds, $p < 0.05$ vs. control) and sustained up to day 11 (2.12 ± 0.19 folds, $p < 0.01$), which corresponded to the early phase of the healing stage (Fig. 2b). In contrast, Cygb protein was significantly increased on days 11 and 18 (1.87 ± 0.13 and 1.60 ± 0.06 folds, respectively, $p < 0.05$), which corresponded to the late phase of healing (Fig. 2c). Interestingly, HIF-1α was not significantly increased on day 18 whereas Cygb was increased. There was a difference between HIF-1α and Cygb protein expression in the time phase.

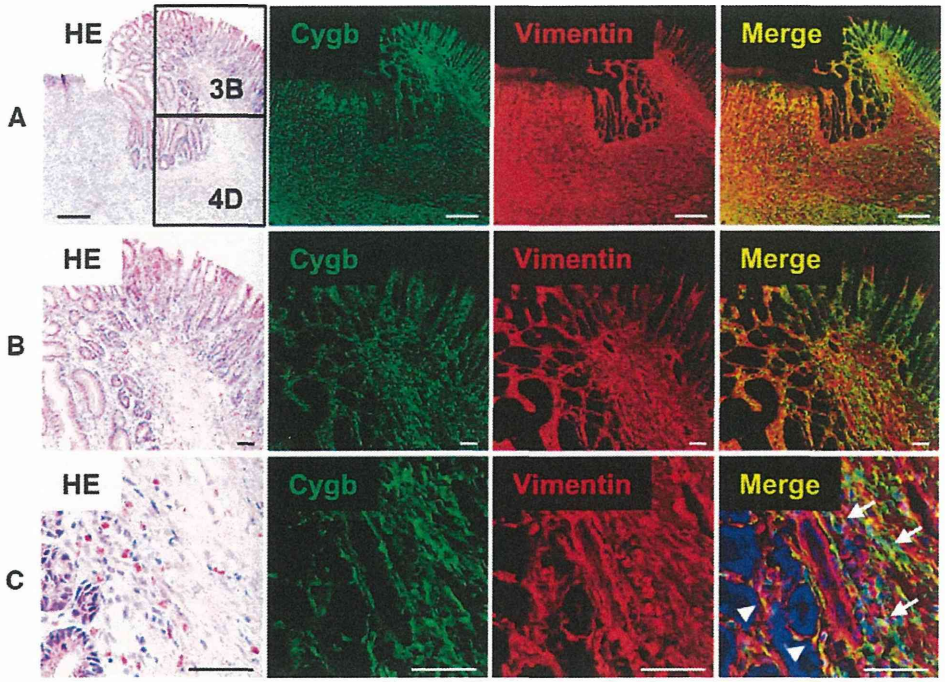

Fig. 3 Localization of Cygb in the ulcerated gastric tissues. **a** Cygb and vimentin expression in the ulcerated area. Cygb and vimentin were colocalized in the cytoplasm of mesenchymal cells in the regenerative area and the ulcer bed. **b** Middle magnified images. Colocalization was observed in the mucosal and submucosal layer. **c** Highly magnified images. Colocalization of Cygb and vimentin was observed in the spindle-shaped cells which were indicated to be fibroblasts (*arrows*). Colocalization was also observed in the linear-shaped cells surrounding the glands which were indicated to be myofibroblasts (*arrowheads*). *HE* hematoxylin and eosin. *Scale bars* **a** 250 μm; **b** and **c** 50 μm

mRNA Expression of HIF-1α and VEGF in the Ulcerated Gastric Tissues

mRNA expression of HIF-1α peaked on day 11 in the time course of ulcer healing (2.29 ± 0.56 folds, $p < 0.05$ vs. control; Fig. 2d). In contrast, VEGF expression was significantly increased on days 11 and 18 (1.02 ± 0.08 and 1.45 ± 0.31 folds, respectively, $p < 0.05$; Fig. 2e). VEGF mRNA expression was gradually increased from day 11 to 18. VEGF expression peaked at day 18.

Localization of Cygb in the Ulcerated Gastric Tissues

On day 11 after the ulcer production, Cygb and vimentin were colocalized in the cytoplasm of mesenchymal cells in the regenerative area and ulcer bed (Fig. 3a). In the regenerative area, immunoreactivity for Cygb was stronger than that in the ulcer bed. Colocalization was observed in the mucosal and submucosal layers (Fig. 3b). On highly magnified images, colocalization was observed in the spindle-shaped cells which were indicated to be fibroblasts (Fig. 3c). Furthermore, colocalization was also observed in the linear-shaped cells surrounding the glands which were indicated to be myofibroblasts. We could confirm the evidence that showed the linear-shaped cells represented myofibroblasts by colocalization of Cygb and α-SMA (Fig. 4a). Cygb was not expressed in the muscle cells which were positive for vimentin and α-SMA. Cygb was also not expressed in the epithelial cells which were immunoreactive for cytokeratin (Fig. 4b).

Localization of Cygb and HIF-1α in the Ulcerated Gastric Tissues

HIF-1α was expressed in the mucosal and submucosal layers at the marginal zone of the ulcer (Fig. 4c). Colocalization of Cygb and HIF-1α was stronger in the submucosal layer than that in the mucosal layer. On highly magnified images, colocalization was observed in the submucosal spindle-shaped cells which were indicated to be fibroblasts. Cygb protein, as well as HIF-1α, was observed at the regenerative tissues where angiogenesis had not developed at that time.

Association of Cygb With/Without Angiogenesis in the Ulcerated Gastric Tissues

The pattern of angiogenesis is different in the regenerative gastric tissues around the ulcer. Immunoreactive cells for Cygb were abundantly present at the regenerative tissues where immunoreactivity of HIF-1α was abundant (Fig. 4c). In contrast, immunoreactive cells for Cygb were sparsely